***PREPRINT**: Blocken B, Carmeliet J. 2006. On the validity of the cosine projection in wind-driven rain calculations on buildings. Building and Environment 41(9): 1182-1189. © Elsevier 2006.*

On the validity of the cosine projection in wind-driven rain calculations on buildings

Bert Blocken [a] *, Jan Carmeliet [a,b]

[a] *Laboratory of Building Physics, Department of Civil Engineering, Katholieke Universiteit Leuven, Kasteelpark Arenberg 40, 3001 Leuven, Belgium*
[b] *Building Physics Group, Faculty of Building and Architecture, Technical University Eindhoven, P.O. box 513, 5600 MB Eindhoven, The Netherlands*

Abstract

Wind-driven rain (WDR) is one of the most important boundary conditions governing the hygrothermal performance and the durability of building facades. Information concerning the quantity of WDR falling onto building facades is an essential requirement as a boundary condition for Heat-Air-Moisture transfer analyses and for building facade design. The quantity of WDR can be calculated with either semi-empirical methods (such as the WDR relationship) or numerical simulation methods that are based on Computational Fluid Dynamics (CFD). The WDR relationship is most often used. It applies the cosine projection to take into account the effect of varying wind direction on the WDR quantity or intensity. Up to now, the validity of the cosine projection for WDR calculations has not yet been investigated. Its use was suggested in the past and it has been adopted for all semi-empirical WDR calculations since then. Also in the recently developed numerical simulation methods, it is tempting to apply the cosine projection to reduce the computational expense. In the present paper, the validity of the cosine projection is investigated based on 3D numerical simulations of WDR with CFD. It will be shown that the cosine projection, although generally accepted, is not strictly valid and that it can give rise to significant errors.

Keywords: Driving rain; Wind flow; Building; Semi-empirical formula; Numerical simulation; CFD; Computational Fluid Dynamics

1. Introduction

Wind-driven rain (WDR) is one of the most important boundary conditions for the study of the hygrothermal performance and the durability of building facades. Knowledge of the quantity of WDR that falls onto building facades is an essential input for Heat-Air-Moisture (HAM) transfer models and for the design of building facades. Therefore, adequate procedures are needed for calculating the quantity or intensity of WDR on different positions on a building facade, preferably from standard available meteorological data: wind speed, wind direction and horizontal rainfall intensity (i.e. the rainfall intensity falling through a horizontal plane, as measured by a traditional rain gauge).

Currently, two categories of methods exist for calculating the quantity or intensity of WDR based on standard meteorological data: (1) semi-empirical methods and (2) numerical simulation methods based on Computational Fluid Dynamics (CFD). A review of each of these methods is given in [1]. The most often used semi-empirical method to calculate the quantity or intensity of WDR on building facades is the WDR relationship, which will be briefly discussed next. The WDR relationship was first suggested by Hoppestad [1, 2]. Originally, it was intended to relate the free-field WDR intensity to the wind speed and the horizontal rainfall intensity. The free-field WDR intensity refers to the intensity of WDR falling

* Corresponding author: Bert Blocken, Laboratory of Building Physics, K.U.Leuven, Kasteelpark Arenberg 40, B-3001 Leuven, Belgium. Tel.: +32 (0) 16-321345 - Fax: +32 (0) 16-321980

through an imaginary vertical plane that is always facing the wind and that is situated in an open field, without any nearby buildings or other obstructions. This relationship is given by Eq. (1):

$$R_{wdr} = \kappa \cdot U \cdot R_h \quad (1)$$

where R_{wdr} is the WDR intensity (mm/h), κ is the free-field WDR coefficient (s/m), U is the reference wind speed (m/s) and R_h is the horizontal rainfall intensity (mm/h). Later, this relationship was refined by Lacy [3, 4] who found a free-field WDR coefficient that was on average equal to $\kappa = 0.222$ s/m. The simplicity of the WDR relationship drove researchers to not only use it for calculating the free-field WDR intensity but to also use it for determining the intensity of WDR falling onto building facades. Therefore, the WDR coefficient α was introduced [Eq. (2)]:

$$R_{wdr} = \alpha \cdot U \cdot R_h \quad (2)$$

This coefficient is different from κ because it takes into account the effect of the building and of other obstructions at the building site as well as the influence of the position on the building wall. The coefficient α is typically determined by WDR measurements on buildings. It is known to vary significantly with the building geometry and with the position on the building facade, but it is generally assumed to be independent of wind speed, wind direction and horizontal rainfall intensity. Eq. (2) is used to calculate the WDR intensity when the wind direction is perpendicular to the building facade. To take into account the effect of varying wind direction on the WDR intensity, the cosine projection is used:

$$R_{wdr} = \alpha \cdot U \cdot R_h \cdot \cos\theta \quad (3)$$

where θ is the angle between the wind direction and the normal to the wall. Note that adding $\cos\theta$ implies that the horizontal, upstream, streamwise velocity vector with magnitude U is projected normal to the wall. Eq. (3) is commonly referred to as “the WDR relationship”, “the WDR formula” or “Lacy’s formula”. All researchers that have been using the WDR relationship for calculating WDR on buildings have also adopted the cosine projection. Note that also the European Standard Draft PrEN 13013-3 [5] for WDR calculation employs the cosine projection.

During the past 15 years, a numerical simulation method for quantifying WDR on building facades has been developed. A steady-state simulation technique was developed and introduced by Choi [6-8] and it was extended and incorporated into a general numerical simulation method by Blocken and Carmeliet [9]. The method was recently validated by comparison with full-scale WDR measurements [9, 10] and it was shown that it can provide accurate indications of the quantity of WDR falling onto the facade of a low-rise building. The numerical simulation method is significantly more powerful and yields more detailed information than the WDR relationship. On the other hand, as opposed to the simplicity of the WDR relationship, the numerical simulation method is complex, time-consuming and computationally expensive. Therefore it is tempting to perform numerical simulations of WDR on building facades only for wind directions perpendicular to the building facades, and to use the cosine projection for the other wind directions.

To the knowledge of the authors, no attempt has been made up to now to investigate the validity of the cosine projection. Since its introduction, it has been used for calculating WDR on building facades without any knowledge of the possible errors involved. In this paper, the validity of the cosine projection in WDR calculations is investigated by means of numerical simulations with CFD. In section 2, first a few definitions and the influencing parameters of WDR are given. Section 3 briefly describes the numerical simulation method for WDR. In section 4, the numerical method is used to calculate the WDR distribution on the facade of a low-rise cubic building model for various wind directions. These numerical simulations will allow investigating the validity of the cosine projection in section 5.

2. Wind-driven rain: definitions and parameters

The quantities that are used to describe the WDR intensity in numerical simulations are the specific catch ratio $\eta_d(d)$, related to the raindrop diameter d, and the catch ratio η, related to the entire spectrum of raindrop diameters [Eq. (4)]:

$$\eta_d(d) = \frac{R_{wdr}(d)}{R_h(d)} \quad ; \quad \eta = \frac{R_{wdr}}{R_h} \tag{4}$$

where $R_{wdr}(d)$ and $R_h(d)$ are the specific WDR intensity and the specific unobstructed horizontal rainfall intensity (for raindrop diameter d). R_{wdr} and R_h are the WDR intensity and the unobstructed horizontal rainfall intensity (integrated over all raindrop diameters). The unobstructed horizontal rainfall intensity is the intensity of rainfall through a horizontal plane that is situated outside the wind-flow pattern that is disturbed by the building (i.e. the rainfall that would be measured by a rain gauge with a horizontal orifice at ground-level, placed in an open field). The catch ratio η is a complicated function of space and time. The six basic influencing parameters for η are: (1) the building geometry (including environment topology), (2) the position on the building facade, (3) the reference wind speed, (4) the reference wind direction, (5) the horizontal rainfall intensity and (6) the horizontal raindrop-size distribution. The reference wind speed U (m/s) is usually taken as the horizontal component of the wind-velocity vector at 10 m height in the upstream undisturbed flow (U_{10}). The reference wind direction φ_{10} (degrees from north) refers to the direction of the reference wind speed. The horizontal raindrop-size distribution $f_h(d)$ (m^{-1}) refers to the raindrop-size distribution as a flux through a horizontal plane.

Note that the catch ratio η is typically used in the numerical WDR simulation method, while the WDR coefficient α is typically used in the semi-empirical WDR relationship. Combining Eq. (3) and (4), it is clear that the both quantities, for $\theta = 0°$, are simply related by the reference wind speed U [Eq. (5)]:

$$\alpha = \frac{R_{wdr}}{U \cdot R_h} = \frac{\eta}{U} \tag{5}$$

3. Numerical wind-driven rain simulation method

The numerical method for the simulation of WDR has been described in detail by Blocken and Carmeliet [9]. In the interest of brevity, only the headlines will be repeated here. This paper will focus on the results of the simulations and on their use to investigate the validity of the cosine projection, rather than on the simulations themselves.

The numerical method for the quantification of the spatial and temporal distribution of WDR on buildings consists of 5 steps:

1. The steady-state 3D wind-flow pattern around the building is calculated using a CFD code. The Reynolds-Averaged Navier-Stokes equations are solved and closure is usually obtained by employing a k-ε turbulence model.
2. Raindrop trajectories are obtained by injecting raindrops of different sizes in the calculated wind-flow pattern and by solving their equation of motion.
3. For several positions on the building facade, the specific catch ratio is determined based on the configuration of the calculated raindrop trajectories in the wind-flow field that ended on the building facade.
4. The catch ratio at these positions is calculated from the specific catch ratio and from the raindrop-size distribution. Catch-ratio charts are constructed for the different positions at the building facade. Examples of such charts will be given in the next section.
5. The meteorological data record of reference wind speed, wind direction and horizontal rainfall intensity for a given rain event is combined with the appropriate catch-ratio charts to determine the corresponding spatial and temporal distribution of WDR on the building facade.

For the present study, only steps 1 to 4 will be used. It is important to note that the numerical wind-driven rain simulation method (including all 5 steps) has been quite extensively validated for a low-rise building of complex geometry [9, 10]. It has been shown that the method can provide an accurate indication of both the spatial and temporal distribution of WDR on the building facade. The confidence in the numerical method that has arisen from these validation studies allows us to use this method and its results for the purpose of this paper.

4. Wind-driven rain simulations on the facade of a cubic building model

The numerical simulation method was applied to determine the distribution of WDR on the facade of a low-rise cubic building model with dimensions lxbxh = 10x10x10 m^3 (Fig. 1).

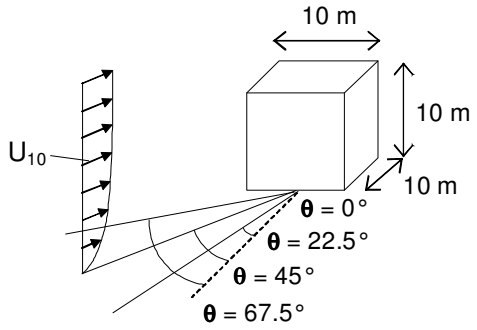

Fig. 1. Low-rise cubic building model (lxbxh = 10x10x10 m³). CFD simulations are conducted for four different wind directions.

The simulations were conducted for various reference wind-speed values (U_{10} = 1, 2, 3, 4, 5, 6, 8, 10 m/s), for various wind directions (θ = 0°, 22.5°, 45°, 67.5°) and for various horizontal rainfall intensities (R_h = 0.1, 0.5, 1, 2, 3, 4, 5, 6, 8, 10, 15, 20, 25, 30 mm/h). The simulations of the wind-flow pattern were performed with the commercial CFD code Fluent 5.4 that employs the control-volume method [11]. The realizable k-ε model [12] and standard wall functions [13] were employed. The calculation of the raindrop trajectories, the specific catch ratio and the catch ratio were performed with author-written program codes. The characteristics and settings of these simulations are given in detail in [14]. In this paper, we limit ourselves to mentioning the following important aspects: (1) The building model stands alone on a large plain covered with short grass (aerodynamic roughness length y_0 = 0.03 m). (2) The dimensions of the computational domain are LxBxH = 310x110x60 m³ and the blockage ratio is about 1.5%. (3) Suitable numerical grids (unstructured, tetrahedral) for each wind direction were obtained based on grid-sensitivity analyses, yielding about 10^6 control volumes for each grid. (4) The wind-flow calculations were performed with a power-law inlet wind-speed profile with an exponent α_P = 0.15, corresponding to y_0 = 0.03 m. (5) The turbulent dispersion of the raindrops is neglected [1,9]. (6) The raindrop-size distribution of Best [15] is adopted. This raindrop-size distribution is characterised by a unique relationship between the horizontal rainfall intensity R_h and the horizontal raindrop-size distribution $f_h(d)$. Let us recall the six basic influencing parameters of the catch ratio mentioned in section 2. Then, for a given building geometry, for a given position on the building facade and adopting the raindrop-size distribution according to Best [15], the catch ratio is unambiguously defined by three parameters: the reference wind speed U_{10}, the wind direction φ_{10} (or θ) and the horizontal rainfall intensity R_h. The results will be presented for different combinations of these three parameters.

Results of the numerical simulations are provided in Fig. 2 and 3. Fig. 2 shows the spatial distribution (contour lines) of the catch ratio η on the windward facade of the building model, for U_{10} = 10 m/s, for R_h = 1 mm/h and for all four different wind directions. The variation of the spatial distribution with the wind direction is briefly described:

1. Fig. 2a (θ = 0°). The spatial distribution is symmetrical. The catch ratio η increases from bottom to top and from the middle of the facade to the vertical edges. The highest values are found at the top edge, with a maximum at the top corners: η = 1.72.
2. Fig. 2b (θ = 22.5°). Compared to Fig. 2a, η increases at the upwind vertical edge (i.e. the left edge, see wind direction in Fig. 1) and decreases at the downwind edge. The highest values are found at

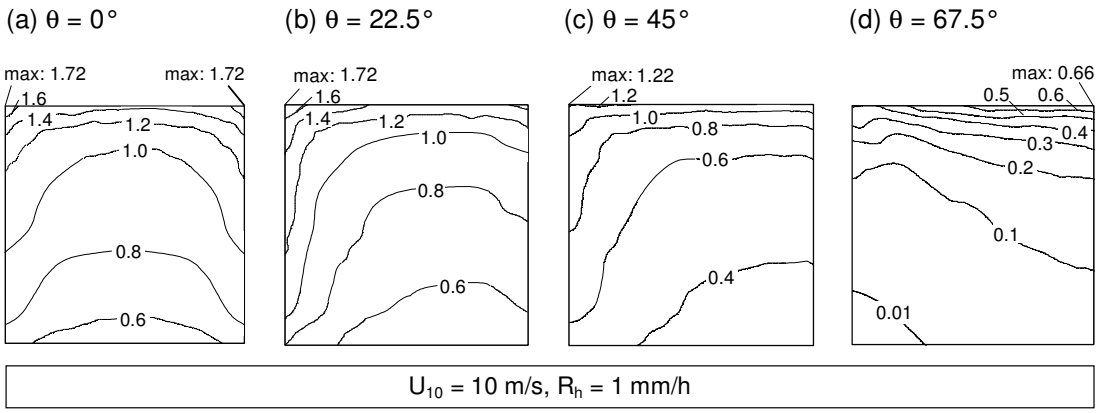

Fig. 2. CFD-simulation results: contours of the catch ratio η on the windward facade of the low-rise cubic building model for U_{10} = 10 m/s, R_h = 1 mm/h and for four different wind directions.

the top edge and at the upper part of the upwind vertical edge. The maximum value is found at the upwind top corner and its value is the same as that for θ = 0°.

3. Fig. 2c (θ = 45°). A general decrease of η is found. The highest values are found at the top edge and at the upper part of the upwind vertical edge. The maximum value is present at the upwind top corner.
4. Fig. 2d (θ = 67.5°). From θ = 45° to θ = 67.5°, the spatial distribution pattern completely changes. There is a large decrease of η across the entire facade surface. The highest values are now situated at the downwind top corner.

In addition to Fig. 2 that only provides information for a fixed value of U_{10} and R_h, Fig. 3 shows catch-ratio charts at position P (middle of the downwind vertical edge) for the four wind directions. The catch-ratio charts display η as a function of U_{10} and R_h. All charts show that the catch ratio increases approximately linearly with wind speed. There is generally a steep increase of η with increasing horizontal rainfall intensity for light horizontal rainfall intensities (R_h < 1 mm/h). It levels out as the horizontal rainfall intensity increases. The influence of the wind direction is clear as a considerable reduction of the values in the charts with increasing wind direction.

5. Examining the validity of the cosine projection

The cosine projection implies that the catch ratio (and hence the WDR intensity) for a wind direction θ can be obtained by multiplying the catch ratio for θ = 0° with the factor cosθ:

$$\eta(U_{10}, R_h, \theta) = \eta(U_{10}, R_h, 0°) \cdot \cos\theta \quad (6)$$

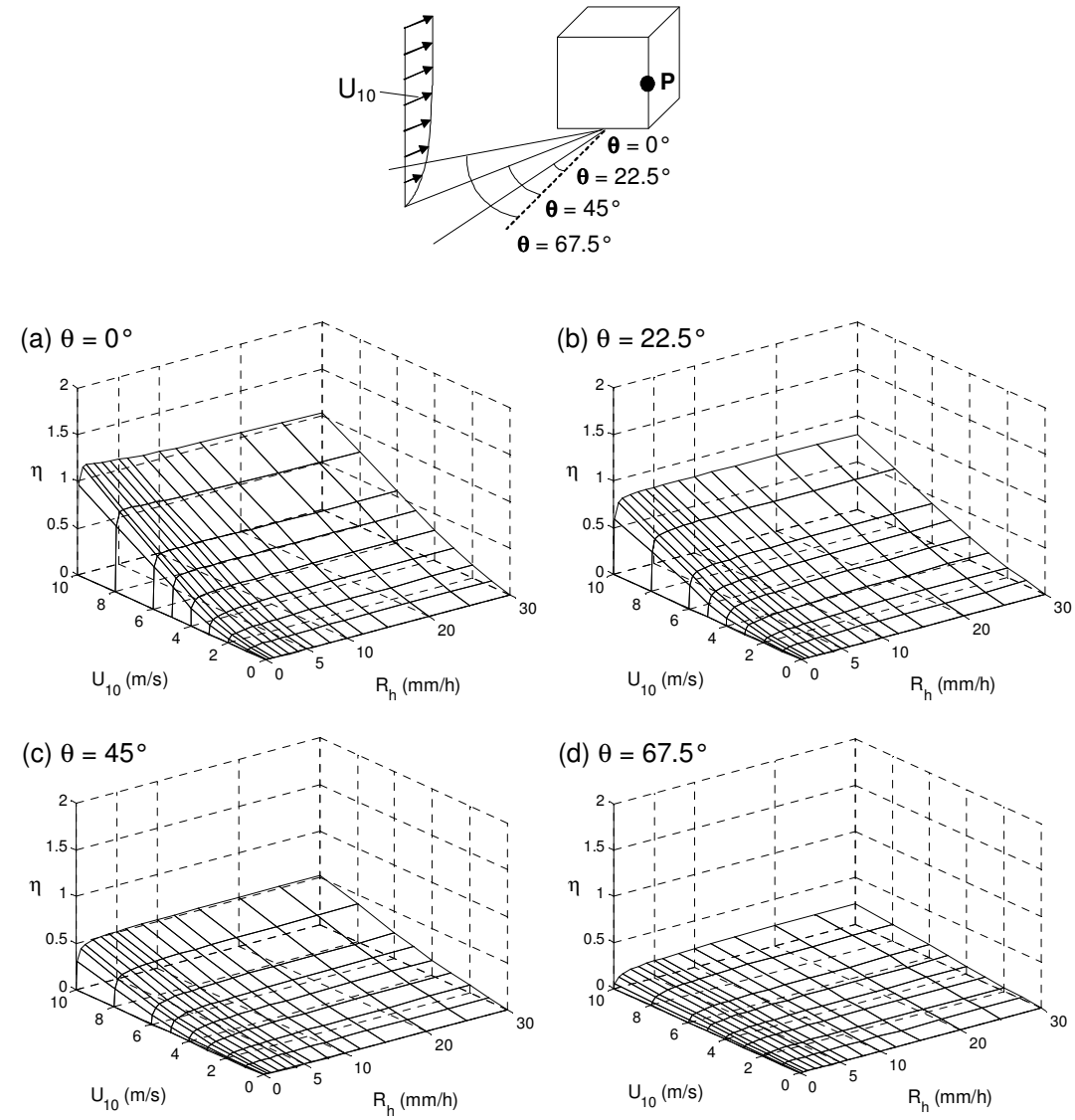

Fig. 3. CFD-simulation results: catch-ratio charts for position P on the windward facade of the cubic building model and for four different wind directions. Each catch-ratio chart displays the catch ratio η as a function of the reference wind speed U_{10} and the horizontal rainfall intensity R_h for a fixed wind direction.

Based on the simulated catch-ratio distribution for $\theta = 0°$ (Fig. 2a), the catch-ratio distributions for the other three wind directions were obtained using Eq. (6). Fig. 4 shows the results. Comparing Fig. 2b-d and Fig. 4b-d shows that the use of the cosine projection is not valid and that it can give rise to significant errors. A significantly different spatial distribution of the catch ratio is obtained. For clarity, Fig. 5 shows the error percentages that are introduced by the use of the cosine projection. The errors were calculated with Eq. (7):

$$e(\theta) = 100 \cdot \frac{\eta(U_{10}, R_h, 0°) \cdot \cos\theta - \eta(U_{10}, R_h, \theta)}{\eta(U_{10}, R_h, \theta)} \tag{7}$$

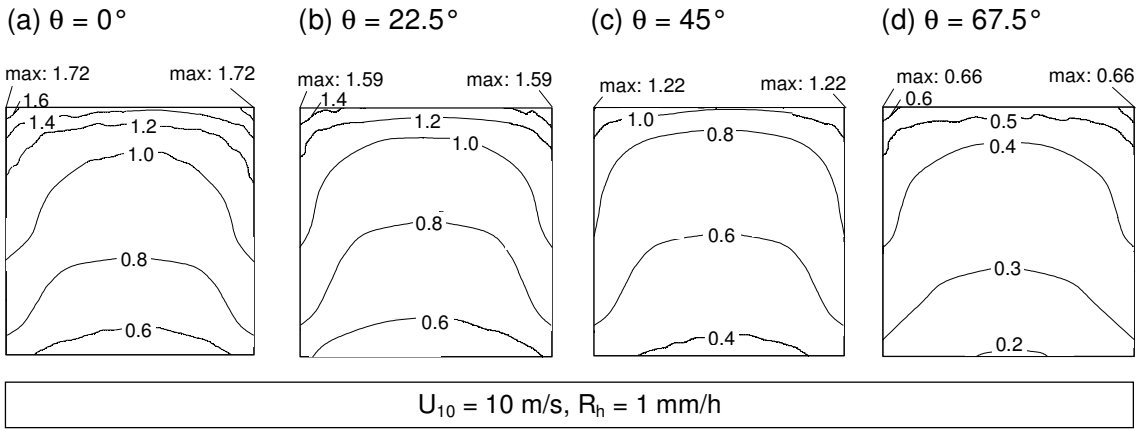

Fig. 4. Results of applying the cosine projection to the CFD result in Fig. 2a. All figures are for U_{10} = 10 m/s and for R_h = 1 mm/h.

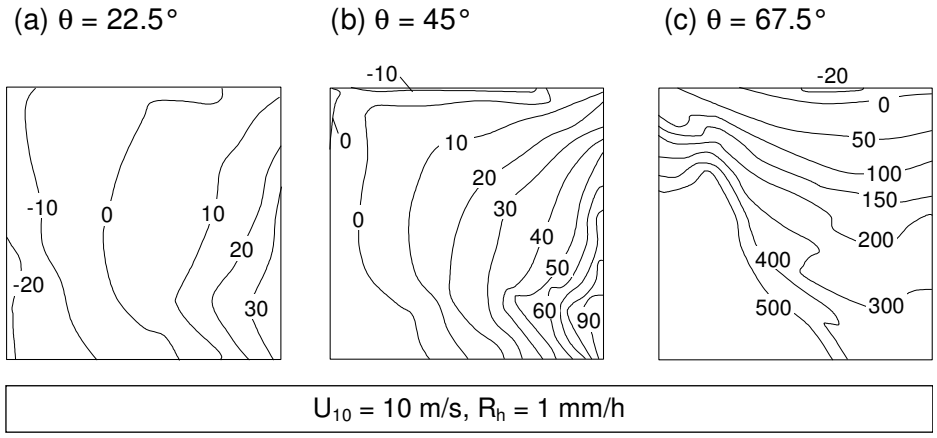

Fig. 5. A graphical presentation of the errors (in percentages) that are introduced by the use of the cosine projection for U_{10} = 10 m/s, R_h = 1 mm/h and for the three wind directions.

Note that all η-values used as input in Eq. (7) are obtained from CFD simulations. The following observations are made from Fig. 5:

1. The distribution of the error on the facade is quite complex. The complexity increases as the wind direction θ increases. This is due to the actual complex variation of the distribution of WDR on a building facade with wind direction as opposed to the simple assumption of the cosine projection.
2. The tendency for general overestimation of the catch ratio by the cosine projection increases as the wind direction θ increases.
3. Fig. 5a (θ = 22.5°). Even for a small deviation of the wind direction from the normal to the wall, the error can amount up to 30%.
4. Fig. 5b (θ = 45°). At the upwind vertical edge and at the top edge, the error is small. At the downwind vertical edge however, very large errors are found.
5. Fig. 5c (θ = 67.5°). Large errors are found at practically all positions of the facade. The largest errors are found at the upwind bottom corner and are due to the small values of $\eta(U_{10}, R_h, \theta)$ at this position (see Fig. 2d).

Fig. 5 only shows errors for U_{10} = 10 m/s and R_h = 1 mm/h. In order to provide some information about the variation of the error with U_{10} and R_h, Fig. 6 shows the distribution of the error by the cosine projection as a function of these variables for position P at the building facade. The following observations are made:

1. The errors increase significantly with increasing wind direction.
2. The largest errors are clearly found for light to moderate horizontal rainfall intensities and for the higher wind-speed values. But even for the heavy rainfall intensities and the lower wind-speed values, the errors remain quite large (several tens of percentages).

6. Discussion and conclusions

The cosine projection is traditionally used in calculations of wind-driven rain on building facades to take into account the effect of varying wind direction on the wind-driven rain intensity. In this paper, the

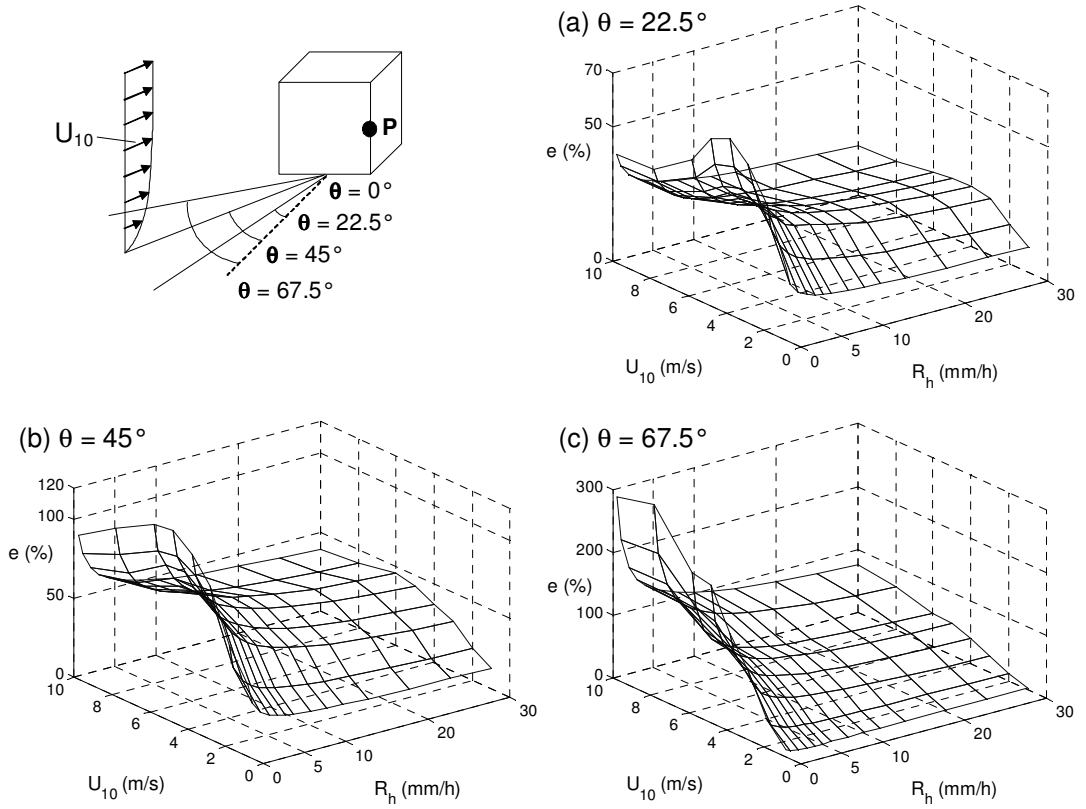

Fig. 6. A graphical presentation of the errors (percentages) that are introduced by the use of the cosine projection at position P of the windward facade. The errors are given as a function of U_{10} and R_h for the three wind directions.

validity of the cosine projection has been investigated with a numerical simulation method for wind-driven rain that is based on Computational Fluid Dynamics. Confirmation about the adequacy and the reliability of the numerical simulation method was obtained by earlier validation studies. Based on simulations for a low-rise cubic building model, it has been illustrated that the cosine projection, although generally adopted and used for all wind-driven rain calculations with semi-empirical methods, is strictly not valid and that it can give rise to significant errors.

The study in this paper has been limited to a simple cubic building model. For more complex building models, the complexity of the wind-flow pattern will increase, which in turn will cause an increased complex wind-driven rain distribution pattern. In such cases, the failure of the cosine projection is likely to be even more pronounced. Further research will focus on the confirmation of this expectation.

The research reported in this paper has been limited to demonstrating the invalid character of the cosine projection. One might argue that future research should focus on the development of an improved

(but still simplified) way to take into account the effect of varying wind direction. Given the complexity of the wetting patterns however, even for a simple cubic building model (see Fig. 2), this might turn out to be a (nearly) impossible task. In that case, dependent on the required accuracy of the calculations, numerical simulation with CFD might be the only option.

Acknowledgements

The first author has held a Ph.D. scholarship of the IWT-Flanders and is currently a post-doctoral research engineer of the FWO-Flanders. The IWT-Flanders (Institute for the Promotion of Innovation by Science and Technology) supports and stimulates research and technology transfer in the Flemish Industry. The FWO-Flanders (Fund for Scientific Research) supports and stimulates fundamental research in Flanders. Their contribution is gratefully acknowledged. We are also grateful for the kind assistance of Wendy Desadeleer during this research work.

References

[1] Blocken B, Carmeliet J. A review of wind-driven rain research in building science. Journal of Wind Engineering and Industrial Aerodynamics 2004;92(13): 1079-1130.
[2] Hoppestad S. Slagregn i Norge (in Norwegian). Norwegian Building Research Institute, rapport Nr. 13, Oslo; 1955.
[3] Lacy RE. Driving-rain maps and the onslaught of rain on buildings. RILEM/CIB Symp. on Moisture Problems in Buildings, Rain Penetration, Helsinki; 1965, Vol. 3, paper 3-4.
[4] Lacy RE. Climate and building in Britain. Her Majesty's Stationery Office, London; 1977.
[5] CEN. Hygrothermal performance of buildings – Climatic data – Part 3: Calculation of a driving rain index for vertical surfaces from hourly wind and rain data. Draft prEN 13013-3; 1997.
[6] Choi ECC. Numerical simulation of wind-driven rain falling onto a 2-D building. Asia Pacific Conference on Computational Mechanics, Hong Kong; 1991. p. 1721-1728.
[7] Choi ECC. Simulation of wind-driven rain around a building. Journal of Wind Engineering and Industrial Aerodynamics 1993;46&47: 721-729.
[8] Choi ECC. Determination of wind-driven rain intensity on building faces. Journal of Wind Engineering and Industrial Aerodynamics 1994;51: 55-69.
[9] Blocken B, Carmeliet J. Spatial and temporal distribution of driving rain on a low-rise building. Wind and Structures 2002;5(5): 441-462.
[10] Blocken B, Carmeliet J. Validation of CFD simulations of wind-driven rain on a low-rise building facade. Journal of Wind Engineering and Industrial Aerodynamics, 2005. Submitted.
[11] Fluent Inc. Fluent 5 User's Guide; 1998.
[12] Shih TH, Liou WW, Shabbir A, Zhu J. A new k-ε eddy-viscosity model for high Reynolds number turbulent flows – model development and validation. Computers and Fluids 1995;24(3): 227-238.
[13] Launder BE, Spalding DB. The numerical computation of turbulent flows. Computer Methods in Applied Mechanics and Engineering 1974;3: 269-289.
[14] Blocken B, Carmeliet J. The influence of the wind-blocking effect on the wind-driven rain exposure of building facades. Journal of Wind Engineering and Industrial Aerodynamics; 2004. Submitted.
[15] Best AC. The size distribution of raindrops. Quarterly Journal of the Royal Meteorological Society 1950;76: 16-36.

FIGURE CAPTIONS

Fig. 1. Low-rise cubic building model (lxbxh = 10x10x10 m³). CFD simulations are conducted for four different wind directions.

Fig. 2. CFD-simulation results: contours of the catch ratio η on the windward facade of the low-rise cubic building model for U_{10} = 10 m/s, R_h = 1 mm/h and for four different wind directions.

Fig. 3. CFD-simulation results: catch-ratio charts for position P on the windward facade of the cubic building model and for four different wind directions. Each catch-ratio chart displays the catch ratio η as a function of the reference wind speed U_{10} and the horizontal rainfall intensity R_h for a fixed wind direction.

Fig. 4. Results of applying the cosine projection to the CFD result in Fig. 2a. All figures are for U_{10} = 10 m/s and for R_h = 1 mm/h.

Fig. 5. A graphical presentation of the errors (in percentages) that are introduced by the use of the cosine projection for U_{10} = 10 m/s, R_h = 1 mm/h and for the three wind directions.

Fig. 6. A graphical presentation of the errors (percentages) that are introduced by the use of the cosine projection at position P of the windward facade. The errors are given as a function of U_{10} and R_h for the three wind directions.